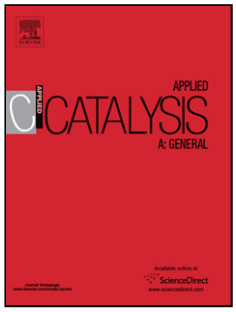

Title: Insight into the hydrogenation of pure and crude HMF to furan diols using Ru/C as catalyst

Authors: Sara Fulignati, Claudia Antonetti, Domenico Licursi, Matteo Pieraccioni, Erwin Wilbers, Hero Jan Heeres, Anna Maria Raspolli Galletti

PII: S0926-860X(19)30159-0
DOI: https://doi.org/10.1016/j.apcata.2019.04.007
Reference: APCATA 17039

To appear in: *Applied Catalysis A: General*

Received date: 1 November 2018
Revised date: 18 March 2019
Accepted date: 8 April 2019

Please cite this article as: Fulignati S, Antonetti C, Licursi D, Pieraccioni M, Wilbers E, Heeres HJ, Galletti AMR, Insight into the hydrogenation of pure and crude HMF to furan diols using Ru/C as catalyst, *Applied Catalysis A, General* (2019), https://doi.org/10.1016/j.apcata.2019.04.007

Insight into the hydrogenation of pure and crude HMF to furan diols using Ru/C as catalyst

Sara Fulignati[a], Claudia Antonetti[a], Domenico Licursi[a], Matteo Pieraccioni[a], Erwin Wilbers[b], Hero Jan Heeres[b], Anna Maria Raspolli Galletti[a,*]

[a] Department of Chemistry and Industrial Chemistry, University of Pisa, Via G. Moruzzi 13, 56124, Pisa, Italy

[b] Green Chemical Reaction Engineering, ENTEG, University of Groningen, Nijenborgh 4, 9747 AG Groningen, The Netherlands

*Corresponding author, e-mail: anna.maria.raspolli.galletti@unipi.it

Graphical abstract

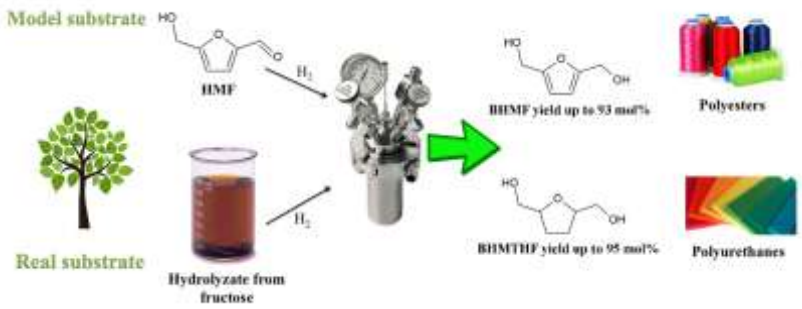

Highlights

- The tunable hydrogenation of both aqueous HMF solutions and crude fructose hydrolyzate to renewable diols BHMF and BHMTHF, was studied.
- 5 wt% Ru/C resulted an active and robust catalyst, showing negligible sintering and leaching processes.
- Yields of BHMF up to 93 mol% and of BHMTHF up to 95 mol% were ascertained starting from aqueous HMF.
- This study proves the feasibility of renewable monomers synthesis from the crude fructose hydrolyzate, opening the way for their production directly from lignocellulosic biomass through a cascade process.

Abstract

5-hydroxymethylfurfural (HMF) is one of the most important renewable platform-chemicals, a very valuable precursor for the synthesis of bio-fuels and bio-products. In this work, the hydrogenation of HMF to two furan diols, 2,5-bis(hydroxymethyl)furan (BHMF) and 2,5-bis(hydroxymethyl)tetrahydrofuran (BHMTHF), both promising renewable monomers, was investigated. Three commercial catalysts, Ru/C, Pd/C and Pt/C, were tested in the hydrogenation of aqueous HMF solutions (2-3 wt%), using a metal loading of 1 wt% respect to HMF content. By appropriate tuning of the process

conditions, either BHMF or BHMTHF were obtained in good yields, and Ru/C resulted the best catalyst for this purpose, allowing us to obtain BHMF or BHMTHF yields up to 93.0 and 95.3 mol%, respectively. This catalyst was also tested for in the hydrogenation of a crude HMF-rich hydrolyzate, obtained by one-pot the dehydration of fructose. The influence of each component of this hydrolyzate on the hydrogenation efficiency was investigated, including unconverted fructose, rehydration acids and humins, in order to improve the yields towards each furan diol. Moreover, ICP-OES and TEM analysis showed that the catalyst was not subjected to important leaching and sintering phenomena, as further confirmed by catalyst recycling study.

Keywords

5-hydroxymethylfurfural; aqueous-phase hydrogenation; 2,5-bis(hydroxymethyl)furan; 2,5-bis(hydroxymethyl)tetrahydrofuran; crude hydrolyzate.

1. Introduction

Nowadays, the dwindling supplies of worldwide fossil resources and the growth of carbon dioxide emission make the production of chemicals and fuels from renewable resources a key topic of the industrial chemistry [1-3]. Biomass is a very promising alternative feedstock, being abundant, cheap, widespread and precursor for the production of several valuable products [4-6]. In particular, 5-hydroxymethylfurfural (HMF) is considered as one of the most important bio-based compounds [7]. HMF may be obtained by the dehydration of model compounds, including monosaccharides, such as glucose [8-11] and fructose [11-15], polysaccharides, such as inulin [12,13,16], starch [11,15] and cellulose [11,15,17,18] and, more advantageously, real lignocellulosic biomasses, such as corn stover, pinewood, switchgrass and poplar [14,19]. The presence of different reactive groups (an aldehyde group, a hydroxyl group and a furan ring) makes HMF a very important platform-chemical, precursor of bio-fuels, such as 2,5-dimethylfuran (DMF) [20,21], 5-ethoxymethylfurfural (EMF) [22] and long chain alkanes [23]. In addition, it is possible to convert HMF into interesting monomers, such as 2,5-furandicarboxylic acid (FDCA) [24,25], 2,5-bis(hydroxymethyl)furan (BHMF) [26-28], 2,5-bis(hydroxymethyl)tetrahydrofuran (BHMTHF) [29-31] and caprolactone [32] and many more valuable products [33-35].

In this work, the selective synthesis of two important furan diols, BHMF and BHMTHF, is investigated. The first one derives from the hydrogenation of the aldehyde group of HMF, whereas the second one stems from the hydrogenation of both aldehyde group and furan ring. Their application for the synthesis of resins, fibres, foams and polymers has been recently proven, underlining their high potential as monomers for the synthesis of alternative and renewable materials [36-40]. Regarding their possible synthesis, the majority of the literature investigations employs molecular hydrogen as reducing agent, in particular for the synthesis of BHMTHF, whereas the hydrogenation of HMF to BHMF

has been also carried out using formic acid [41] or isopropanol [42,43] as hydrogen donor, or through electrochemical processes [28]. Concerning the catalyst selection, mainly heterogeneous catalysts have been used and only a few papers have described the use of homogeneous ones [41, 44]. Advantages of the former are ease of separation from the reaction medium and recyclability. The most largely adopted heterogeneous catalysts are represented by metals, such as Ru, Pt, Pd, Au, Ir, Ni, Cu supported on several oxides, polymers or carbon species [3,30,36,45-53]. Ru-, Pd-, and Pt-catalysts are particularly attractive for this purpose, because of their high intrinsic activity, and it is usually easy to have them dispersed as nanoparticles on an appropriate support [53]. In most of the published works, the HMF hydrogenation has been carried out working with toxic, expensive, and non-renewable solvents, such as ionic liquids and organic solvents (mainly tetrahydrofuran, 1,4-dioxane and alcohols). However, from a green chemistry point of view, the use of water is certainly preferred. In addition, the HMF upgrading in water is of more practical importance, because HMF is expected to be directly supplied as an aqueous solution in a biorefinery process, thus minimizing or, even better, avoiding expensive and unnecessary purification steps. Unfortunately, lower diols selectivities are reported when the reaction is performed in water, rather than in organic or biphasic solvent systems [30,54,55]. In fact, water-based HMF hydrogenation may lead to different products, because this reaction environment could enable the hydrolytic ring opening, the hydrodeoxygenation and rearrangements of the furan ring. On this basis, the selectivity of the water-based hydrogenation of HMF to BHMF and BHMTHF is markedly determined by the hydrogenation activity and acid–base properties of the chosen catalytic system. Functional sites determine the selectivity of products in a catalytic reaction system for the hydrogenation of HMF in water, using supported metal catalysts, in particular the metal surface for hydrogenation/hydrogenolysis, the support surface for acid–base catalysis, the metal-support interface for the unique adsorption of

reactants, and the acid–base catalysis, determined by the presence of water and other compounds of the reaction mixture. Focusing the attention on the catalysts of interest in this work, the best results in aqueous medium have been obtained using non-commercial, *ad hoc* synthesized catalysts. In this regard, Chen et al. [46] carried out the hydrogenation of diluted aqueous HMF solution employing Ru clusters immobilized on nanosized mesoporous zirconium silica (Ru/MSN-Zr) as catalyst, reaching the maximum BHMF yield of 90 mol%. They have also investigated the synthesis of BHMTHF from HMF in water [48] adopting Pd catalyst supported on amine-functionalized metal-organic frameworks (Pd/MIL-101(Al)-NH_2), obtaining the BHMTHF yield of 96 mol%. Despite the promising catalytic performances of many *ad hoc* synthetised catalysts, some problems still limit their application on a larger scale, such as the reproducibility of catalyst formulation (and therefore of its properties), the cost of recovery of the precious metal from the spent catalyst after its use, the cost of the support and catalyst production. Commercial catalysts still remain the preferred choice for hydrogenation reactions, in particular those carbon-based, because of their lower cost, high surface area, chemical inertness, thermal stability in non-oxidizing atmospheres, and ease of metal recovery, allowed by simple calcination. The use of commercial catalysts for the synthesis of the diols was reported by Schiavo et al. [57]. A wide range of noble metals supported on carbon, such as 10 wt% Pd/C, 10 wt% Pt/C and 10 wt% Ru/C, was tested together with Raney Ni, platinum oxide and copper chromite. All catalysts were active towards the HMF hydrogenation in water to BHMF and BHMTHF and, particularly, 10 wt% Ru/C showed promising results, by properly tuning the reaction time. In particular, the BHMF yield of 95 mol% was obtained after 30 min, whereas prolonging the reaction to 4 h gave the BHMTHF yield of 92 mol%. These results were obtained adopting a low HMF concentration (1.3 wt%), which could be responsible of the ascertained good selectivity. Moreover, the authors did not perform a systematic investigation and they did not study

the influence of the main reaction parameters to give the target diols. Regarding the possible role of the catalytic support, Alamillo et al. [30] proved that acidic supports, such as SiO_2, have a detrimental role on the HMF hydrogenation, favouring the selective formation of ring opening triols and tetrol, such as 1,2,5-hexanetriol, 1,2,5,6-hexanetetrol and 1,2,6-hexanetirol, formed by the hydrogenation of acid-catalyzed degradation products of BHMF. In this context, also the presence of other homogeneous acids, which are typical of the hydrolyzate solutions, such as H_2SO_4 and levulinic acid, also caused a significant reduction of furan diols selectivity. These statements suggest that the pH of the aqueous reaction solution has certainly a strong influence on the furan diols selectivity and, in particular, a low pH causes undesired ring opening and also degradation of HMF and reaction intermediates, leading to the undesired formation of humins. This issue could be partially solved on laboratory scale by using a biphasic system, which allows HMF extraction from the aqueous phase, minimizing its degradation to acids and humins. This application is still academically interesting, even if not very practical from an industrial point of view. In this context, Alamillo et al. [30] studied the activity of Ru black in different solvents and the highest BHMTHF selectivity (67 mol%) at complete HMF conversion was obtained using tetrahydrofurfuryl alcohol, whereas it markedly decreased to 46 mol% employing the biphasic water/1-butanol (1/2 v/v) system and even more in water (22 mol%). The decrease of BHMTHF yield was attributed to the formation of polyols, such as 1,2,6-hexanetriol and 1,2,5-hexanetriol, deriving from the hydration of the intermediate BHMF, together with additional degradation pathways occurring in water. In addition to the acid–base properties of a reaction system, also the hydrogenation rate has an influence on the yield or selectivity of BHMF and BHMTHF, because BHMF is relatively unstable under hydrothermal reaction conditions. In this sense, the maximum yield of BHMF can be obtained by increasing the hydrogenation rate of HMF beyond that of BHMF ring opening. On the basis of the above statements, HMF hydrogenation in

water is certainly challenging for industrial applications, but very difficult to tune, depending on the contribute of many different components, which simultaneously act within the reaction environment, and which must be individually and experimentally considered, for a better understanding of the reaction.

Starting from the work of Schiavo et al. [30], in this work, the hydrogenation of more concentrated HMF aqueous solution (2-3 wt%) has been carried out in the presence of commercial noble metals supported on carbon, Ru/C, Pd/C and Pt/C. The choice of carbon support for this purpose is appropriate, thanks to its relative inertness, which prevents the occurrence of unwanted reactions catalyzed by the support surface acidity, thus allowing us to focus the attention on the sole effect of the reaction mixture. The adopted HMF concentration was similar to that reached in water for crude HMF synthesis from fructose hydrolysis, previously optimized by us [13]. The BHMF and BHMTHF yields have been optimized by properly tuning the process conditions, in order to minimize the ring opening issue. These optimized reaction conditions have been subsequently employed in the cascade process for the direct hydrogenation of the HMF-rich crude hydrolyzate obtained from the dehydration of fructose to HMF, without any intermediate separation step. With this approach, the intermediate separation and purification steps to obtain pure HMF are avoided, because unnecessary, with a positive impact on the techno-economic viability of the overall process from fructose to renewable furan diols.

2. Methods

2.1 Materials

5-hydroxymethylfurfural (95%) was supplied by AVA Biochem. 2,5-bis(hydroxymethyl)furan (95%) and 2,5-bis(hydroxymethyl)tetrahydrofuran (95%) were provided by AKos GmbH (Germany). Ru/C (5 wt%), Pd/C (5 wt%), formic acid (99.8%),

levulinic acid (98%), ethanol (96%), dichloromethane (99.9%), sodium bicarbonate and water for HPLC were purchased from Sigma-Aldrich. Pt/C (5 wt%) was supplied by Strem Chemicals. Fructose was food grade. Amberlyst-70 was provided by Rohm and Haas. All catalysts and chemicals were employed as received.

2.2 Hydrogenation of HMF

Hydrogenation reactions were carried out in a 300 mL stainless steel Parr 4560 autoclave equipped with a P.I.D. controller (4843). In a typical experiment, a weight ratio metal to HMF of 1 wt% was used. In this regard, the catalyst employed as received, was weighted and introduced into the autoclave, which was subsequently closed and evacuated to 65 Pa with a mechanical vacuum pump. 50 mL of a HMF aqueous solution was introduced into the autoclave by suction, and the reaction mixture was stirred using a mechanical overhead stirrer. Then, the reactor was pressurized with hydrogen till the desired pressure was reached at the pre-set temperature, always under mechanical stirring. The pressure in the reactor was manually held constant at the pre-determined value by repeated hydrogen addition, when necessary. The reaction progress was monitored by sampling periodically the liquid through a dip tube. The liquid samples were analysed using HPLC. All the experiments were carried out in triplicate and the reproducibility of the techniques was within 3%. For the recycling tests, the employed catalyst was recovered by filtration and re-used within two subsequent runs. At the end of the third cycle, the recovered catalyst was washed with acetone, dried and re-used for an additional recycling test.

2.3 Synthesis of a HMF-rich hydrolyzate from fructose

The hydrolyzate was prepared using a microwave reactor CEM Discover S-class System, according to the procedure reported by Antonetti et al. at optimum reaction conditions [13]. At the end of the hydrolysis reaction, the heterogeneous catalyst Amberlyst-70 was separated by the liquid fraction through centrifugation, and the isolated liquid fraction was employed as raw feedstock of the subsequent hydrogenation.

2.4 Hydrogenation of hydrolyzate with Ru/C

The hydrogenation of the HMF-rich hydrolyzate from fructose was conducted analogously to that of pure HMF and, also in this case, a weight ratio metal to HMF of 1 wt% was adopted. The progress of the reaction was monitored by sampling periodically the liquid through a dip tube. The liquid samples were analyzed by HPLC.

2.5 Analytical equipment

2.5.1 High-Pressure Liquid Chromatography

High-pressure liquid chromatography (HPLC) analysis of the liquid samples deriving from HMF hydrogenation runs was carried out with Perkin Elmer Flexer Isocratic Platform equipped with a column Benson 2000-0 BP-OA (300 mm x 7.8 mm). A 0.005 M H_2SO_4 aqueous solution was adopted as mobile phase, maintaining the column at 60 °C with a flow-rate of 0.6 mL/min. The concentrations of products were determined from calibration curves obtained with standard solutions. Conversion, products yield and products selectivity were expressed in mol%. The carbon balance was evaluated as the sum of the moles of products and unconverted HMF respect to the initial moles of HMF and it was expressed in mol%.

2.5.2 Gas Chromatography coupled with Mass Spectrometer

The by-products formed during the hydrogenation of HMF were qualitatively identified by gas chromatography coupled with mass spectrometer (GC-MS). Before the analysis, the aqueous solution was extracted with dichlorometane. A GC-MS (Agilent 7890B-5977A) equipped with HP-5MS capillary column (30 m × 0.25 mm × 0.25 μm) (5%-phenyl)-methylpolysiloxane was employed for the analysis. The carrier gas was helium with a flow of 1 mL/min. The injector and detector temperatures were 250 °C and 280 °C, respectively. The following temperature program was adopted for the chromatographic run: 70 °C isothermal for 2 min; 12 °C/min up to 250 °C; 250 °C isothermal for 2 min.

2.5.3 Transmission Electron Microscopy

Transmission Electron Microscopy (TEM) measurements in bright field mode were conducted with a CM12 microscope (Philips), operating at 120 keV. The catalysts were suspended in ethanol by ultra-sonication, and the obtained sample was dropped onto carbon coated 400 mesh copper grids. Images were taken on a slow scanning CCD camera. The ruthenium particle size distribution was evaluated by measuring at least 100 particles with the software Nano Measurer 1.2.

2.5.4 Nitrogen physisorption

Nitrogen physisorption experiments were carried out in a Micromeritics ASAP 2020 at −196.2 °C. Before the measurement, the samples were degassed under vacuum at 150 °C for 6 h. The surface area was estimated using the standard BET method. The single point desorption total pore volume (VT) was calculated from the amount of gas adsorbed at a relative pressure of 0.98 in the desorption branch.

2.5.5 Thermogravimetric analysis

Thermogravimetric analysis (TGA) of the fresh and used catalysts was determined using a TGA Q50 system (TA Instrument). The samples were heated in a nitrogen atmosphere, employing a temperature range between 20 and 650 °C, and a heating rate of 10 °C/min.

2.5.6 Inductively coupled plasma-optical emission spectrometry

Inductively coupled plasma-optical emission spectrometry (ICP-OES) was employed to determine the metal content in the catalyst after reaction using an Optima 7000 DV (PerkinElmer) analyser equipped with a CCD array detector. Sample digestion was carried out in a microwave oven (CEM MARS 5). 20 mg of catalyst was weighted and introduced in the vessel together with a mixture of HNO_3 (7 mL), HCl (1 mL) and HF (2 mL). The vessel was closed and heated at 200 °C for 2 h. Subsequently, the vessel was cooled to room temperature and diluted to 50 mL with double-distilled water, prior to the ICP-OES analysis.

2.5.7 Gas-phase analysis

The Micro-GC Agilent 3000 equipped with a thermal conductivity detector was employed for the CO identification. The channel used for CO analysis was the molecular sieve column Molsieve 5A (10 m x 0.32 mm x 12 μm), adopting argon as carrier gas.

3. Results and discussion

3.1 Metal species screening

Starting from the work of Schiavo et al. [30], a preliminary screening of the catalytic performances of different commercial catalysts (Ru/C, Pd/C and Pt/C, 5 wt%) was performed at 140 °C, 70 bar H_2, with the initial HMF concentration of 2 wt% and the metal to HMF ratio of 1 wt%. The results are reported in Table 1.

Table 1, near here

Pt/C resulted the least active system and the HMF conversion was only 64.5 mol% after 1 h of reaction. Both Pd/C and Ru/C were more active and complete HMF conversion was reached after 1 h. Regarding products distribution, Pt/C gave a very low selectivity to BHMF (< 16 mol%). GC-MS analysis of the reaction mixture (Figure S1) showed the presence of several by-products deriving from the hydrodeoxygenation of HMF, such as 2,5-hexanedione, 5-methyl-2-furaldehyde and 5-hydroxy-2-hexanone (Scheme 1A), in agreement with the literature [58].

Scheme 1, near here

Under the adopted reaction conditions, Pt/C mainly promotes the hydrodeoxygenation and ring opening of HMF, resulting in a poor selectivity towards the desired furan diols. On the other hand, both Pd/C and Ru/C favour hydrogenation reactions, leading to improved BHMTHF yields (55.8 and 88.6 mol% for Pd/C and Ru/C, respectively). Among the three catalysts, Ru/C is surely the most promising, combining high HMF conversion with high BHMTHF selectivity, as also confirmed by the best carbon balance, the closest to 90 mol%. In this case, only minor amounts of by-products were detected,

such as tetrahydrofurfuryl alcohol, 5-methyl-tetrahydrofurfuryl alcohol, 2,5-dimethyltetrahydrofuran and tetrahydro-2H-pyran-2-methanol. These are known by-products, deriving from BHMTHF degradation reactions which are promoted at elevated temperatures [59] (Figure S2 and Scheme 1B). For Pd/C catalyst, not only the hydrogenation of both aldehyde group and furan ring of HMF occurs, but also hydrodeoxygenation and ring opening reactions (Scheme 1C), as ascertained by the presence of typical by-products, such as 5-methyl-tetrahydrofurfuryl alcohol, 2,5-hexanedione, 5-hydroxy-2-hexanone and 1,2,6-hexanetriol (Figure S3), in agreement with the literature [55,60,61].

On the basis of this exploratory screening, Ru/C was identified as the most promising commercial catalyst for the aqueous hydrogenation of HMF to the target diols, and therefore it was adopted for subsequent optimization studies.

3.2 Optimization of BHMF and BHMTHF yields in the presence of Ru/C

The above reported preliminary screening has been performed under harsh reaction conditions (140 °C and 70 bar H_2). Subsequently, in order to improve the selectivity of the reaction, milder reaction conditions have been adopted, in terms of temperature and H_2 pressure. In particular, the influence of temperature (100-140 °C) on the catalytic performances at 70 bar H_2 was investigated, and the obtained results are reported in Figure 1.

Figure 1, near here

The conversion of HMF was almost complete already at short reaction time (30 min), for all the adopted temperatures. On the other hand, temperature strongly influenced the products distribution. In fact, at 140 °C (Figure 1A), the amount of BHMF was negligible during the whole reaction due to the extensive hydrogenation of the furan ring and BHMTHF yield of 79.3 mol% was ascertained after 30 min. BHMTHF yield reached the maximum value of 88.6 mol% after 60 min, and then decreased, due to the formation of

by-products, as evidenced by the corresponding trend of carbon balance (run 4, Table S1). Working at 120 °C (Figure 1B), the hydrogenation of the furan ring was slower and, after 30 min, the BHMF yield of 16.0 mol% was obtained. The maximum BHMTHF yield shifted from 60 to 180 min (Figures 1A and 1B), when it resulted higher than that ascertained at 140 °C, reaching 92.8 mol%. These results underline that the by-products formation is favoured at high temperature, as confirmed by the corresponding trend of carbon balance at the different temperatures reported in Table S1, and by the results obtained decreasing the reaction temperature up to 100 °C (Figure 1C). In fact, in this last case, the BHMTHF yield continuously increased with the time, reaching the highest value of 95.0 mol% after 240 min.

On this basis, the effect of the decrease of H_2 pressure to 50 bar was further investigated working at 100 °C, and the obtained results are reported in Table 2.

Table 2, near here

The decrease of H_2 pressure did not influence the HMF conversion, that resulted almost complete (compare runs 7 and 8, Table 2) during the whole reaction. On the other hand, at short reaction time (30 min), the lower pressure led to a higher BHMF yield at the expense of BHMTHF yield, due to the reduced hydrogenation of the furan ring.

The concentration of the starting feedstock is another very important parameter because, usually, high substrate concentrations promote side-reactions, and the yields and/or selectivities towards target products fall down. The initial HMF concentration was increased from 2 to 3 wt% (runs 8 and 9, Table 2) at 50 bar H_2, on the basis of the HMF concentration obtained from fructose in a previous study adopting Amberlyst A-70 as acid catalyst in water [13], in the perspective of a feasible cascade approach.

The presence of a higher amount of the initial substrate did not limit the hydrogenation of the aldehyde group of HMF, whose conversion resulted unchanged, but caused a slowdown of the furan ring hydrogenation, as evidenced in particular at short reaction

times. However, at the end of the reaction, analogous BHMTHF yields were ascertained starting from 2 and 3 wt% HMF solutions. Moreover, in order to prove the key role of Ru/C towards the activation of the HMF hydrogenation, a blank run without the catalyst was performed under the same reaction conditions (100 °C, 50 bar H_2, 3 wt% HMF solution). In this case, after 240 min, the conversion of HMF resulted 10.6 mol% and only BHMF in trace was detected, confirming the necessity of employing a suitable catalyst for the hydrogenation of HMF. In conclusion, the highest BHMTHF yield of 95.3 mol% was reached starting from 3 wt% HMF aqueous solution at 100 °C, 50 bar H_2 after 240 min. This represents a very promising result, considering that BHMTHF yields over 90 mol% have been reported working only on less concentrated water solution, adopting higher H_2 pressures [56,57], and/or higher temperatures [57], longer reaction times [48,57] and, in the presence of *ad hoc* synthetized catalysts, which are not still really interesting for industrial applications in the immediate future.

Once having optimized the synthesis of BHMTHF, this study was focused on the optimization of BHMF synthesis, where the sole hydrogenation of the aldehyde group of HMF is required. The above results suggested that it was necessary to adopt milder reaction conditions and thus, the H_2 pressure was reduced to 30 bar (run 10, Table 2). The hydrogenation of HMF was slowed down and, for the first time, its conversion was not complete within the first hour of reaction. As a consequence, also the hydrogenation of the furan ring was limited, causing the increase of BHMF yield, which resulted 79.5 mol% after 30 min. However, under the H_2 pressure of 30 bar, BHMF underwent other side-reactions, as evidenced by the worsening of the carbon balance in run 10, reaching the value of 29.6 mol%, after 240 min. The pressure of 30 bar H_2 was not sufficient to promote the hydrogenation of the furan ring, which requires high temperatures and high pressures to occur [53]. However, as reported in the literature [59,62], at high temperatures and low pressures, the ring opening of BHMF prevailed, resulting faster

than the hydrogenation of the furan ring. In fact, the low hydrogen pressure is disadvantageous for hydrogen solubilisation in water, inhibiting the conversion of BHMF to BHMTHF, and promoting the formation of partially hydrogenated products, which are intermediates for the synthesis of polyols, such as 1,2,6-hexanetriol, 1,2-hexanediol, 1,6-hexanediol, 1-hydroxyl-2,5-hexanedione and 1,2,5-hexanetriol [30, 59]. In fact, as reported in the literature, 1,2,6-hexanetriol derives from the ring opening of BHMF and hydrogenation of the intermediate, whereas 1,2-hexanediol and 1,6-hexanediol originate from the break of the C-O bond of C6 or C2 of 1,2,6-hexanetriol, respectively [59]. Regarding 1-hydroxyl-2,5-hexanedione and 1,2,5-hexanetriol, the first one derives from the rearrangement of BHMF, favoured in water, followed by ring opening, whereas 1,2,5-hexanetriol is the product of 1-hydroxyl-2,5-hexanedione complete hydrogenation [30]. In order to optimize the BHMF production, the investigation of temperature within the range 50-120 °C was carried out at 30 bar H_2, and the results are reported in Figure 2.

Figure 2, near here

As expected, HMF conversion increased with temperature, which strongly influences the distribution of products. In fact, when the reaction was performed at 50 °C, the BHMF yield continuously increased, reaching the highest value of 93.0 mol%, after 240 min. When the temperature was raised to 70 °C, the maximum of the BHMF yield (90.0 mol%) shifted to shorter reaction time (120 min), and then it strongly decreased by prolonging the reaction. The further increase of the reaction temperature, first to 100 °C and then to 120 °C, promoted the BHMF decomposition, as confirmed also by the progressive decrease of carbon balance (runs 13 and 14, Table S2).

Therefore, the highest BHMF yield (93.0 mol%) was reached on 3 wt% HMF aqueous solution at 50 °C, 30 bar H_2, and after 240 min, with a Ru/HMF ratio of 1 wt% (run 11).

In the literature, analogous BHMF yields are reported starting from aqueous HMF solutions only employing significantly less sustainable reaction conditions [27,45,46,57].

3.3 Hydrogenation of crude HMF-rich hydrolyzate obtained from fructose dehydration

The synthesis of BHMF and BHMTHF starting from pure HMF is scarcely attractive in an industrial perspective due to the high cost of HMF, caused by its low yield in both production and purification steps. On this basis, the hydrogenation of a crude HMF-rich hydrolyzate was also investigated, thus evaluating the effect of other compounds, which are typical of a real HMF-rich hydrolyzate, on the catalytic performances towards the next HMF hydrogenation step. The hydrolyzate was obtained from the dehydration of fructose, according to our previous work, in the presence of the commercial resin Amberlyst-70 as acid catalyst, and the best HMF yield of 45.6 mol% was reached [13]. At the end of the hydrolysis reaction, the catalyst was separated by filtration and the hydrolyzate was composed of 3 wt% of HMF, 2 wt% of unreacted fructose, 0.08 wt% of formic acid and 0.15 wt% of levulinic acid, showing a pH=2.6, due to the significant presence of the organic acids. This real hydrolyzate was subjected to hydrogenation at 100 °C and 50 bar H_2 (Figure 3, run 15).

Figure 3, near here

Comparing the above reaction profile with that of the hydrogenation of pure HMF, which was carried out under the same reaction conditions (run 9, Table 2), it is evident that, starting from the real hydrolyzate, the HMF conversion and the yields of the diols were significantly lower than those achieved starting from pure HMF. This is due to the significant formation of by-products, as confirmed by the very low carbon balance (run 15, Table S3). These include the unconverted fructose, rehydration acids, formic and levulinic ones, and soluble humins. In order to verify the influence of these compounds on the hydrogenation performances, some model mixtures, having the typical concentrations of the raw hydrolyzate, were prepared, thus separately investigating the

effect of the addition of these components on the HMF hydrogenation. In this regard, four model mixtures were prepared and hydrogenated: 1) HMF (3 wt%) with fructose (2 wt%) (Figure 4A, run 16); 2) HMF (3 wt%) with formic acid (0.08 wt%) and levulinic acid (0.15 wt%) (Figure 4B, run 17); 3) HMF (3 wt%) with formic acid (0.08 wt%) (Figure 4C, run 18); 4) HMF (3 wt%) with levulinic acid (0.15 wt%) (Figure 4D, run 19).

Figure 4, near here

The HMF hydrogenation in the presence of fructose (Figure 4A) proceeded similarly to that of pure HMF (run 10, Table 2), showing that the presence of the unreacted monosaccharide had no influence on the cascade reaction. On the contrary, formic and levulinic acids had a detrimental effect on the hydrogenation of HMF, causing a significant decrease of the reaction rate and a marked drop of BHMF and BHMTHF yields, which respectively reached only 10 and 5 mol% after 30 and 120 min, respectively (Figure 4B). As before evidenced, this result is in agreement with the literature. In fact, not only the acid conditions promote the decomposition of the furan diols [30,57], but it is known the strong deactivating adsorption of formic acid, which remained in the reaction mixture because its decomposition to CO/CO_2 was not significant under the adopted mild conditions [63]. This peculiar behaviour of formic acid was also confirmed comparing the catalyst performances in the hydrogenation of the HMF model mixtures with formic (Figure 4C) or levulinic acids (Figure 4D). In fact, in the presence of formic acid, the conversion of HMF was slower than that found in the HMF hydrogenation with levulinic acid. This is in agreement with the literature results, already reported for the hydrogenation of levulinic acid, where it is underlined that formic acid can be easily and strongly adsorbed on Ru particles in its formate form, limiting the availability of the active sites for the substrate [63-65]. The deactivation of the catalyst, due to the presence of formic acid, was also evidenced by the products formation. In fact, in Figure 4C the conversion of HMF did not lead to diols but rather to other by-products, indicating that

the hydrogenation of HMF was strongly limited. On the other hand, in the presence of levulinic acid (Figure 4D), considerable amount of BHMF was obtained at short reaction time, proving that the HMF hydrogenation occurred, but the acidity of the mixture had a detrimental effect with prolonging the reaction, causing the decreasing of the furan diols yields. Moreover, the formation of humins, deriving from HMF acid condensation [12,13,66], contributed to the catalyst surface passivation [67]. Their formation was confirmed by the very low carbon balance ascertained during the whole reaction in the presence of rehydration acids (runs 17, 18 and 19, Table S3). However, the conversion of HMF reached in the raw hydrolyzate was even lower than that starting from the model mixtures of HMF with rehydration acids, due to the presence of soluble humins already present in the raw hydrolyzate.

In order to overcome this drawback, the raw hydrolyzate was neutralized with $NaHCO_3$ until pH = 7, and then subjected to hydrogenation at 100 °C and 50 bar H_2 (Figure 5).

Figure 5, near here

The neutralization gave an improvement of the catalytic performances, and the BHMF yield markedly improved, reaching the value of 73.2 mol% respect to the starting amount of HMF. This value corresponds to a BHMF yield of 33.4 mol% respect to the starting fructose employed in this cascade approach, being the yields of HMF from fructose in the hydrolysis step equal to 45.6 mol% [13]. However, comparing this run with the hydrogenation of pure HMF (run 9, Table 2), HMF conversion (Figure 5) and the carbon balance (run 20, Table S3) for the neutralized hydrolyzate resulted still lower, and the major product was BHMF, instead of BHMTHF, underlining that the hydrogenation reaction remained almost limited. This evidence can be justified taking into account that the neutralizing step counteracted the acid conditions, responsible for the ring opening by-products and further humins formation in the hydrogenation step, but the passivation

effect of soluble humins already present in the hydrolyzate remained, thus limiting the hydrogenation reaction [67].

Regarding the reaction mechanism of HMF hydrogenation, it is well-known in the literature that Ru-based catalysts favor the hydrogenation of C=O to give 2,5-bis(hydroxymethyl)furan at relatively low temperatures, which would further be converted to 2,5-dimethylfuran via hydrogenolysis, occurring at relatively high temperatures, with 5-methylfurfuryl alcohol and 2,5-hexanedione as intermediate and by-product, respectively [68]. Moreover, regarding the reactivity of HMF, literature studies on aldehydes have shown that decarbonylation path takes place on metals of groups 8, 9, and 10, including ruthenium, especially at high temperatures, leading to the formation of furfuryl alcohol and CO [60]. On the basis of our data, in order to experimentally confirm the HMF hydrogenation mechanism as the main one responsible for the production of BHMF and BHMTHF performed under mild reaction conditions, 50 °C, 30 bar H_2 and 100 °C, 50 bar H_2 respectively, the reaction mixtures obtained under these conditions starting from pure HMF were analysed by GC-MS and the gas-phase reaction products by GC analysis. Only trace amounts of products deriving from hydrogenolysis or decarbonylation reactions of HMF and/or of BHMF, and/or from subsequent hydrogenation/hydrogenolysis reactions on the obtained hydrogenolysis or decarbonylation products were detected (Figure S4 and S5). These products can include 5-methylfurfural, furfuryl alcohol, 5-methylfurfuryl alcohol, 5-methyltetrahydrofurfuryl alcohol, 2,5-dimethyltetrahydrofuran, tetrahydrofurfuryl alcohol, some of which were present in low amounts (not negligible) when the reaction was performed at 140 °C, 70 bar H_2, as already reported in Figure S2, confirming that hydrogenolysis and decarbonylation pathways become more important at high temperatures. Also in the gas-phase, only trace amounts of CO were detected, in agreement with the literature, highlighting as the hydrogenation mechanism is the main one for ruthenium catalysts in

the production of BHMF and BHMTHF from HMF [68]. In this regard, it is reasonable that, when the C=O hydrogenation is the main reaction pathway, the preferential HMF adsorption mode on the active metal occurs in the η^2(C,O)-aldehyde configuration. By this way, BHMF could be selectively formed from this η^2(C,O) species,. Once BHMF was obtained in the reaction mixture, this molecule may be adsorbed in two different modes for the subsequent hydrogenation step: parallel and tilted. The parallel mode may lead to complete hydrogenation, forming BHMTHF, whereas the tilted one may cause the ring opening, through the C-O bond cleavage, with the final formation of 1,2,6-hexanetriol, after hydrogenation step. This proposed mechanism is reported in the Scheme 2, and it is in agreement with the literature data [59,60].

Scheme 2, near here

In order to better evaluate the amount of carbonaceous material on the catalyst surface at the end of the reaction and how it affects the physical properties of the employed catalyst, TGA (Figure 6) and N_2 physisorption (Figure S6 and Table S4) analyses were carried out on fresh and spent Ru/C catalysts at the end of hydrogenation reactions performed adopting different starting materials: solutions of pure HMF (run 9, Table 2), the raw hydrolyzate (run 15, Figure 3) and the neutralized one (run 20, Figure 5).

Figure 6, near here

Figure 6 shows that the amount of carbonaceous material (humins) on the spent catalysts is strongly influenced by the type of the starting substrate. In fact, when the raw hydrolyzate was employed as starting material, the lowest residual weight was acquired at the end of the analysis, confirming that, in this case, the highest amount of humins was deposited on the catalyst, originating from both the crude hydrolyzate and the HMF condensation that took place during the hydrogenation reaction. The neutralizing step allowed the reduction of humins formation, thus the residual weight recorded at the end of the analysis was higher than that obtained for the crude hydrolyzate, but lower than

that for the catalyst employed in the hydrogenation of pure HMF. This explains the trend found for HMF conversion and it is in agreement with the N_2 physisorption experiments reported in Figure S6 and Table S4. In fact, the isothermal curves and the specific surface area values show that the surface area of the spent catalysts depend on the adopted substrate, following this order: pure HMF (153 m^2/g) > neutralized hydrolyzate (62 m^2/g) > raw hydrolyzate (6 m^2/g), being equal to 770 m^2/g that of fresh Ru/C system. The catalyst support plays a significant influence on the catalytic activity in the selective hydrogenation of HMF. The obtained catalytic trend is in agreement with the literature: supports with high surface area favor the dispersion of active metal particles on their surfaces, providing more active catalytic sites for the hydrogenation reactions [36]. Moreover, it is evident that the surface area of the catalyst recovered after the hydrogenation of pure HMF was lower than that of the fresh Ru/C, indicating that, also in this case, some organic material could be adsorbed on the catalyst surface, as previously observed by the comparison of the thermogravimetric curves of these two catalysts reported in Figure 6.

In order to improve the yields towards BHMTHF starting from the crude HMF, harsher reaction conditions (140 °C, 70 bar H_2) were adopted, and the results are shown in Figure 7 (run 21).

Figure 7, near here

Both HMF conversion and carbon balance were similar to those obtained working at 100 °C and 50 bar H_2, but the product distribution significantly changed. In fact, in this case, the prevailing furan diol resulted BHMTHF, which after 240 min reached the yield of 81.1 mol% respect to the amount of initial HMF present in the hydrolyzate, which corresponds to the value of 37.0 mol% respect to the starting fructose, taking into account that in the first step the yield of HMF starting from fructose was 45.6 mol% [13].

Up to now, only few papers report the synthesis of these diols directly from fructose [31,50,69,70]. However, to the best of our knowledge, in this work, for the first time, both fructose dehydration and hydrolyzate hydrogenation were carried out in water instead of organic solvents, ionic liquids or organic-water mixtures. In particular, the first step of this cascade approach is the most critical, due to the possible decomposition of HMF to humins and rehydration acids, which causes the lowering of the HMF yield respect to those obtained with different solvent systems, which should allow an almost quantitative HMF yield [7]. Therefore, in the second step (HMF hydrogenation), the literature investigations performed in organic solvent are based on hydrolyzates which don't include the presence of rehydration acids and humins, thus allowing the maximization of the furan diols yields. However, the employment of organic media or ionic liquid makes the literature processes significantly less sustainable under economic, environmental and safety points of view.

3.4 Catalyst stability

When a heterogeneous catalyst is employed, the evaluation of its stability is an essential issue. For this purpose, the fresh and spent Ru/C catalysts recovered at the end of the optimized reactions for the synthesis of both BHMTHF (run 9, Table 2) and BHMF (run 11, Figure 2), both starting from pure HMF were analysed through ICP-OES and TEM techniques. The first one proved that the leaching of ruthenium in the solution was negligible when it was employed for the synthesis of BHMF and BHMTHF. The TEM pictures and the distributions of the ruthenium particles size for the fresh and the spent Ru/C catalysts are reported in Figure 8.

Figure 8, near here

The TEM image of fresh Ru/C catalyst shows that this system is characterized by ruthenium particles with very small average size, 1.5 nm, in agreement with the results reported in the literature [71]. On the other hand, the ruthenium particles sizes in the spent

catalysts were 2.5 and 2.3 nm, for those employed for the synthesis of BHMTHF and BHMF, respectively. In order to investigate the recyclability of the catalyst, the catalytic system employed in run 9 (Table 2) was recovered at the end of the reaction by filtration, and reused in two subsequent tests, using the same reaction conditions adopted in run 9. The obtained results are reported in Figure 9.

Figure 9, near here

During these three cycles (1, 2 and 3), a slight decrease of the catalytic activity was observed. In fact, the HMF conversion was not complete in the recycling runs and, after the third one, a decrease of 13.8 mol% was obtained. Moreover, a modest increase of BHMF yield (4.2 mol% in the third cycle) was observed, due to the passivation of catalyst surface. At the end of the third cycle, the recovered catalyst was washed with acetone, dried and reused again in another subsequent recycling test. After the washing treatment, the catalyst performances were almost entirely restored, proving that the increase of ruthenium particle sizes did not influence the catalytic activity and confirming that the adopted washing treatment represents an efficient and simple reactivation method, able to remove humins from catalyst surface.

These results underline that catalytic performances of the Ru/C catalyst can be restored, in agreement with our previous research on hydrogenation of raw biomass-derived levulinic acid to γ-valerolactone (GVL) [65], or to 2-methyltetrahydrofuran, and to 2-butanol [72]. The prevailing deactivation of the catalyst can be related only to humin deposition on the surface, which could be removed through washing and/or thermal treatments.

4. Conclusion

Ru/C, Pd/C and Pt/C catalysts were studied in the hydrogenation of pure HMF aqueous solutions to obtain the furan diols 2,5-bis(hydroxymethyl)furan (BHMF) and 2,5-bis(hydroxymethyl)tetrahydrofuran (BHMTHF). Under the same reaction conditions,

Pt/C and Pd/C promoted the HMF hydrodeoxygenation and ring opening, whereas Ru/C mainly activated the HMF hydrogenation, thus resulting as the best catalyst, in terms of conversion and selectivity, towards the desired products. The investigation on Ru/C catalyst revealed that mild reaction conditions were appropriate for obtaining high BHMF yield, whereas higher temperature and H_2 pressure were necessary to hydrogenate also the furan ring, thus selectively obtaining BHMTHF. From the composition of the reaction mixtures, in terms of ascertained by-products, informations on the reaction mechanism were inferred. The hydrogenation of HMF-rich hydrolyzate obtained from the dehydration of fructose aqueous solution was subsequently studied. The investigation evidenced the detrimental role of formic and levulinic acids, which promote the formation of ring opening by-products and humins, which can passivate the catalyst surface. However, the neutralization of the hydrolyzate allowed the improvement of the catalyst performances, preventing the humins formation, as confirmed by N_2 physisorption and TGA analyses of spent catalysts. These results evidence, for the first time, the feasibility of the BHMF and BHMTHF synthesis with good yields, starting from aqueous crude HMF and commercial Ru/C catalyst. Moreover, the recycling data obtained in batch reactor are promising and experiments in continuous set-up are now in progress in order to investigate the catalyst performances for long time on stream.

References

[1] I.K.M. Yu, D.C.W. Tsang, Biores. Technol. 238 (2017) 716-732.

[2] C. Antonetti, D. Licursi, S. Fulignati, G. Valentini, A.M. Raspolli Galletti, Catalysts 6 (2016) 196-224.

[3] L. Hu, L. Lin Z. Wu, S. Zhou, S. Liu, Renew. Sust. Energ. Rev. 74 (2017) 230-257.

[4] D.P. Serrano, J.A. Melero, G. Morales, J. Iglesias, P. Pizarro, Catal. Rev. 60 (2018) 1-70.

[5] C. Antonetti, E. Bonari, D. Licursi, N. Nassi o Di Nasso, A.M. Raspolli Galletti, Molecules 20 (2015) 21232-21253.

[6] A. Galia, B. Schiavo, C. Antonetti, A.M. Raspolli Galletti, L. Interrante, M. Lessi, O. Scialdone, M.G. Valenti, Biotechnol. Biofuels 8 (2015) 218-236.

[7] S.P. Teong, G. Yi, Y. Zhang, Green Chem. 16 (2014) 2015-2026.

[8] M. Li, W. Li, Y. Lu, H. Jameel, H. Chang, L. Ma, RSC Adv. 7 (2017) 14330-14336.

[9] B. Agarwal, K. Kailasam, R.S. Sangwan, S., Elumalai, Renew. Sust. Ener. Rev., 82 (2018) 2408-2425.

[10] A.A. Marianou, C.M. Michailof, A. Pineda, E.F. Iliopoulou, K.S. Triantafyllidis, A.A. Lappas, Appl. Catal. A: Gen. 555 (2018) 75-87.

[11] L. Atanda, A. Shrotri, S. Mukundan, Q. Ma, M. Konarova, J. Beltramini, ChemSusChem 8 (2015) 2907-2916.

[12] C. Antonetti, M. Melloni, D. Licursi, S. Fulignati, E. Ribechini, S. Rivas, J.C. Parajó, F. Cavani, A.M. Raspolli Galletti, Appl. Catal. B: Env. 206 (2017) 364-377.

[13] C. Antonetti, A.M. Raspolli Galletti, S. Fulignati, D. Licursi, Catal. Commun. 97 (2017) 146-150.

[14] A.N. Chermahini, H. Hafizi, N. Andisheh, M. Saraji, A. Shahvar, Res. Chem. Intermed. 43 (2017) 5507-5521.

[15] I.A. Masiutin, A.A. Novikov, A.A. Litvin, D.S. Kopitsyn, D.A. Beskorovaynaya, E.V. Ivanov, Starch/Stärke 68 (2016) 637-643.

[16] X. Qi, M. Watanabe, T.M. Aida, R.L. Smith Jr., Green Chem. 12 (2010) 1855-1860.

[17] H. Shirai, S. Ikeda, E.W. Qian, Fuel Process. Technol. 159 (2017) 280-286.

[18] R. Weingarten, A. Rodriguez-Beuerman, F. Cao, J.S. Lutherbacher, D.M. Alonso, J.A. Dumesic, G.W. Huber, ChemCatChem 6 (2014) 2229-2234.

[19] Y. Yang, C.W. Hu, M.M. Abu-Omar, ChemSusChem 5 (2012) 405-410.

[20] M.J. Gilkey, D.G. Vlachos, B. Xu, Appl. Catal. A: Gen. 542 (2017) 327-335.

[21] J. Li, J. Liu, H. Liu, G. Xu, J. Zhang, J. Liu, G. Zhou, Q. Li, Z. Xu, Y. Fu, ChemSusChem 10 (2017) 1436-1447.

[22] G. Raveendra, A. Rajasekhar, M. Srinivas, P.S. Sai Prasad, N. Lingaiah, Appl. Catal. A: Gen. 520 (2016) 105-113.

[23] B.O. De Beeck, M. Dusselier, J. Geboers, J. Holsbeek, E. Morré, S. Oswald, L. Giebeler, B.F. Sels, Energy Environ. Sci. 8 (2015) 230-240.

[24] G. Yi, S.P. Teong, Y. Zhang, Green Chem. 18 (2016) 979-983.

[25] D.X. Martínez-Vargas, J.R. De La Rosa, L. Sandoval-Rangel, J.L. Guzmán-Mar, M.A. Garza-Navarro, C.J. Lucio-Ortiz, D.A. De Haro-Del Río, Appl. Catal. A: Gen. 547 (2017) 132-145.

[26] G. Bottari, A.J. Kumalaputri, K.K. Krawczyk, B.L. Feringa, H.J. Heeres, K. Barta, ChemSusChem 8 (2015) 1323-1327.

[27] M. Chatterjee, T. Ishizaka, H. Kawanami, Green Chem. 16 (2014) 4734-4739.

[28] J.J. Roylance, T.W. Kim, K. Choi, ACS Catal. 6 (2016) 1840-1847.

[29] N. Perret, A. Grigoropoulos, M. Zanella, T.D. Manning, J.B. Claridge, M.J. Rosseinsky, ChemSusChem 9 (2016) 521-531.

[30] R. Alamillo, M. Tucker, M. Chia, Y. Pagán-Torres, J. Dumesic, Green Chem. 14 (2012) 1413-1419.

[31] H. Cai, C. Li, A. Wang, T. Zhang, Catal. Today 234 (2014) 59-65.

[32] T. Buntara, S. Noel, P.H. Phua, I. Melián-Cabrera, J.G. De Vries, H.J. Heeres, Angew. Chem. Int. Ed. 50 (2011) 7083–7087.

[33] T. Buntara, I. Melián-Cabrera, Q. Tan, J.L.G. Fierro, M. Neurock, J.G. De Vries, H.J. Heeres, Catal. Today 210 (2013) 106-116.

[34] K. Gupta, R.K. Rai, S.K. Singh, ChemCatChem 10 (2018) 2326-2349

[35] B. Ma, Y. Wang, X. Guo, X. Tong, C. Liu, Y. Wang, X. Guo, Appl. Catal. A: Gen. 552 (2018) 70-76.

[36] X. Tang, J. Wei, N. Ding, Y. Sun, X. Zeng, L. Hu, S. Liu, T. Lei, L. Lin, Renew. Sust. Ener. Rev. 77 (2017) 287-296.

[37] M. Gomes, A. Gandini, A.J.D. Silvestre, B. Reis, J. Polym. Sci. Part A: Polym. Chem. 49 (2011) 3759-3768.

[38] D. Zhang, M. Dumont, J. Polym. Sci., Part A: Polym. Chem. 55 (2017) 1478-1492.

[39] L. Hu, J. Xu, S. Zhou, A. He, X. Tang, L. Lin, J. Xu, Y. Zhao, ACS Catal. 8 (2018) 2959-2980.

[40] A. Gandini, T.M. Lacerda, A.J.F. Carvalho, E. Trovatti, Chem. Rev. 116 (2016) 1637-1669.

[41] T. Thananatthanachon, T.B. Rauchfuss, ChemSusChem 3 (2010) 1139-1141.

[42] T. Wang, J. Zhang, W. Xie, Y. Tang, D. Guo, Y. Ni, Catalysts 7 (2017) 92-99.

[43] L. Hu, M. Yang, N. Xu, J. Xu, S. Zhou, X. Chu, Y. Zhao, Korean J. Chem. Eng. 35 (2018) 99-109.

[44] T. Pasini, G. Solinas, V. Zanotti, S. Albonetti, F. Cavani, A. Vaccari, A. Mazzanti, S. Ranieri, R. Mazzoni, Dalton Trans. 43 (2014) 10224-10234.

[45] J. Ohyama, A. Esaki, Y. Yamamoto, S. Arai, A. Satsuma, RSC Adv. 3 (2013) 1033-1036.

[46] J. Chen, F. Lu, J. Zhang, W. Yu, F. Wang, J. Gao, J. Xu, ChemCatChem 5 (2013) 2822-2826.

[47] J. Han, Y.H. Kim, H.S. Jang, S.Y. Hwang, J. Jegal, J.W. Kim, Y.S. Lee, RSC Adv. 6 (2016) 93394-93397.

[48] J. Chen, R. Liu, Y. Guo, L. Chen, H. Gao, ACS Catal. 5 (2015) 722-733.

[49] Y. Nakagawa, K. Takada, M. Tamura, K. Tomishige, ACS Catal. 4 (2014) 2718-2726.

[50] P.P. Upare, Y.K. Hwang, D.W. Hwang, Green Chem. 20 (2018) 879-885.

[51] Y. Zhu, X. Kong, H. Zheng, G. Ding, Y. Zhu, Y.W. Li, Catal. Sci, Technol. 5 (2015) 4208-4217.

[52] X. Kong, Y. Zhu, H. Zheng, F. Dong, Y. Zhu, Y.W. Li, RSC Adv. 4 (2014) 60467-60472.

[53] S. Chen, R. Wojcieszak, F. Dumeignil, E. Marceau, S. Royer, Chem. Rev. 18 (2018) 11023–11117.

[54] F. Liu, M. Audemar, K. De Oliveira Vigier, J.M. Clacens, F. De Campo, F. Jérôme, Green Chem. 16 (2014) 4110-4114.

[55] X. Hu, S. Kadarwati, Y. Song, C.Z. Li, RSC Adv. 6 (2016) 4647-4656.

[56] Y. Nakagawa, K. Tomishige, Catal. Commun. 12 (2010) 154-156.

[57] V. Schiavo, G. Descotes, J. Mentech, Bull. Soc. Chim. Fr. 128 (1991) 704-711.

[58] J. Luo, L. Arroyo-Ramirez, R.J. Gorte, AIChE 61 (2015) 590-597.

[59] S. Yao, X. Wang, Y. Jiang, F. Wu, X. Chen, X. Mu, ACS Sustainable Chem. Eng. 2 (2014) 173-180.

[60] D.P. Duarte, R. Martínez, L.J. Hoyos, Ind. Eng. Chem. Res. 55 (2016) 54-63.

[61] J. Mitra, X. Zhou, T. Rauchfuss, Green Chem. 17 (2015) 307-313.

[62] B. Zhang, Y. Zhu, G. Ding, H. Zheng, Y. Li, Green Chem. 14 (2012), 3402-3409.

[63] H. Heeres, R. Handana, D. Chunai, C.B. Rasrendra, B. Girisuta, H.J. Heeres, Green Chem. 11 (2009) 1247-1255.

[64] A.M. Ruppert, M. Jędrzejczyk, O. Sneka-Płatek, N. Keller, A.S. Dumon, C. Michel, P. Sautet, J. Grams, Green Chem. 18 (2016) 2014–2028.

[65] S. Rivas, A.M. Raspolli Galletti, C. Antonetti, D. Licursi, V. Santos, J.C. Parajó, Catalysts 8 (2018) 169-184.

[66] G. Tsilomelekis, M.J. Orella, Z. Lin, Z. Cheng, W. Zheng, V. Nikolakis, D.G. Vlachos, Green Chem. 18 (2016) 1983-1993.

[67] Y. Yang, Q. Liu, D. Li, J. Tan, Q. Zhang, C. Wang, L. Ma, RSC Adv. 7 (2017), 16311-16318.

[68] L. Hu, X. Tang, J. Xu, Z. Wu, L. Lin, S. Liu, Ind. Eng. Chem. Res. 53 (2014) 3056-3064.

[69] X. Xiang, J. Cui, G. Ding, H. Zheng, Y. Zhu, Y. Li, ACS Sustainable Chem. Eng. 4 (2016) 4506-4510.

[70] W. Zhao, W. Wu, H. Li, C. Fang, T. Yang, Z. Wang, C. He, S. Yang, Fuel 217 (2018) 365-369.

[71] S. Iqbal, S.A. Kondrat, D.R. Jones, D.C. Schoenmakers, J.K. Edwards, L. Lu, B.R. Yeo, P.P. Wells, E.K. Gibson, D.J. Morgan, C.J. Kiely, G.J. Hutchings, ACS Catal. 5 (2015) 5047-5059.

[72] D. Licursi, C. Antonetti, S. Fulignati, M. Giannoni, A.M. Raspolli Galletti, Catalysts 8 (2018) 277-292.

Caption for Figures and Schemes

Fig. 1. Influence of temperature on the HMF aqueous hydrogenation in the presence of 5 wt% Ru/C carried out at 70 bar H_2 and: A) 140 °C (run 4); B) 120 °C (run 5), C) 100 °C (run 6). Reaction conditions: [HMF] = 2 wt%; Ru/HMF = 1 wt%; P H_2 = 70 bar.

Fig. 2. Influence of temperature on the HMF aqueous hydrogenation in the presence of 5 wt% Ru/C carried out at 30 bar H_2 and: 50 °C (run 11); 70 °C (run 12); 100 °C (run 13) and 120 °C (run 14). Reaction conditions: [HMF] = 3 wt%; Ru/HMF = 1 wt%; P H_2 = 30 bar.

Fig. 3. Profile of HMF aqueous hydrogenation of hydrolyzate in the presence of 5 wt% Ru/C (run 15). Reaction conditions: [HMF] = 3 wt%; Ru/HMF = 1 wt%; T = 100 °C; P H_2= 50 bar.

Fig. 4. Profile of HMF aqueous hydrogenation in the presence of 5 wt% Ru/C of: A) fructose + HMF (run 16); B) formic acid + levulinic acid + HMF (run 17); C) HMF + formic acid (run 18); D) HMF + levulinic acid (run 19). Reaction conditions: [HMF] = 3 wt%; Ru/HMF = 1 wt%; T = 100 °C; P H_2= 50 bar.

Fig. 5. Profile of HMF aqueous hydrogenation of neutralized hydrolyzate in the presence of 5 wt% Ru/C (run 20). Reaction conditions: [HMF] = 3 wt%; Ru/HMF = 1 wt%; T = 100 °C; P H_2= 50 bar.

Fig. 6. TGA analysis of fresh and spent Ru/C catalysts recovered at the end of the hydrogenation reactions starting from different initial substrates: pure HMF (run 9, Table 2), hydrolyzate (run 15, Figure 3) and neutralized hydrolyzate (run 20, Figure 5). Reaction conditions: [HMF] = 3 wt%; Ru/HMF = 1 wt%; T = 100 °C; P H_2= 50 bar; t = 240 min.

Fig. 7. Kinetic profile of neutralized hydrolyzate hydrogenation. Reaction conditions: [HMF] = 3 wt%; Ru/HMF = 1 wt%; T = 140 °C; P H_2= 70 bar (run 21).

Fig. 8. TEM pictures of fresh Ru/C (A) and spent Ru/C catalysts employed in run 9, Table 2 (B) or run 11 (C) with the respective distribution of the Ru particles sizes and the Gaussian fitting.

Fig. 9. Hydrogenation of pure HMF in the presence of 5 wt% Ru/C (run 9, Table 2) and four recycles of the solid catalyst.

Scheme 1. Pathways of HMF hydrogenation by-products formation in the presence of the following catalysts: A) Pt/C; B) Ru/C and C) Pd/C.

Scheme 2. Mechanism of HMF hydrogenation.

Table 1 Catalytic performances of commercial systems in the aqueous hydrogenation of HMF. Reaction conditions: [HMF] = 2 wt%; metal/HMF ratio = 1 wt%; T = 140 °C; P H_2= 70 bar; t = 60 min.

Run	Catalyst	HMF Conversion (mol%)	BHMF Yield (mol%)	BHMF Selectivity (mol%)	BHMTHF Yield (mol%)	BHMTHF Selectivity (mol%)	Carbon balance (mol%)
1	**Pt/C (5 wt%)[a]**	64.5	10.7	16.6	0	0	46.2
2	**Pd/C (5 wt%)[b]**	100	0	0	55.8	55.8	55.8
3	**Ru/C (5 wt%)[c]**	100	0	0	88.6	88.6	88.6

[a] Main by-products: 5-methyl-2-furaldehyde; 2,5-hexanedione; 5-hydroxy-2-hexanone.

[b] Main by-products: tetrahydrofurfuryl alcohol; 5-methyl-tetrahydrofurfuryl alcohol; 2,5-dimethyltetrahydrofuran; tetrahydro-2H-pyran-2-methanol.

[c] Main by-products: 5-methyl-tetrahydrofurfuryl alcohol; 2,5-hexanedione; 5-hydroxy-2-hexanone; 1,2,6-hexanetriol.

Table 2 Influence of H_2 pressure and HMF concentration on the aqueous hydrogenation of HMF in the presence of 5 wt% Ru/C. Reaction conditions: Ru/HMF ratio = 1 wt%; T = 100 °C.

Run	P H_2 (bar)	[HMF] (wt%)	HMF Conversion (mol%)				BHMF Yield (mol%)				BHMTHF Yield (mol%)				Carbon Balance (mol%)			
			Time (min)															
			30	60	120	240	30	60	120	240	30	60	120	240	30	60	120	240
7	70	2	97.0	100	100	100	22.2	0.0	0.0	0.0	69.3	87.0	90.1	95.3	94.5	87.0	90.1	95.3
8	50	2	96.8	100	100	100	32.0	0.0	0.0	0.0	59.2	89.3	91.8	93.3	94.4	89.3	91.8	93.3
9	50	3	96.8	100	100	100	71.3	16.9	0.0	0.0	25.0	71.5	92.0	95.3	99.5	88.4	92.0	95.3
10	30	3	89.5	98.4	100	100	79.5	64.4	21.2	0.0	2.9	6.1	19.2	29.6	92.9	72.1	40.4	29.6

Scheme 1

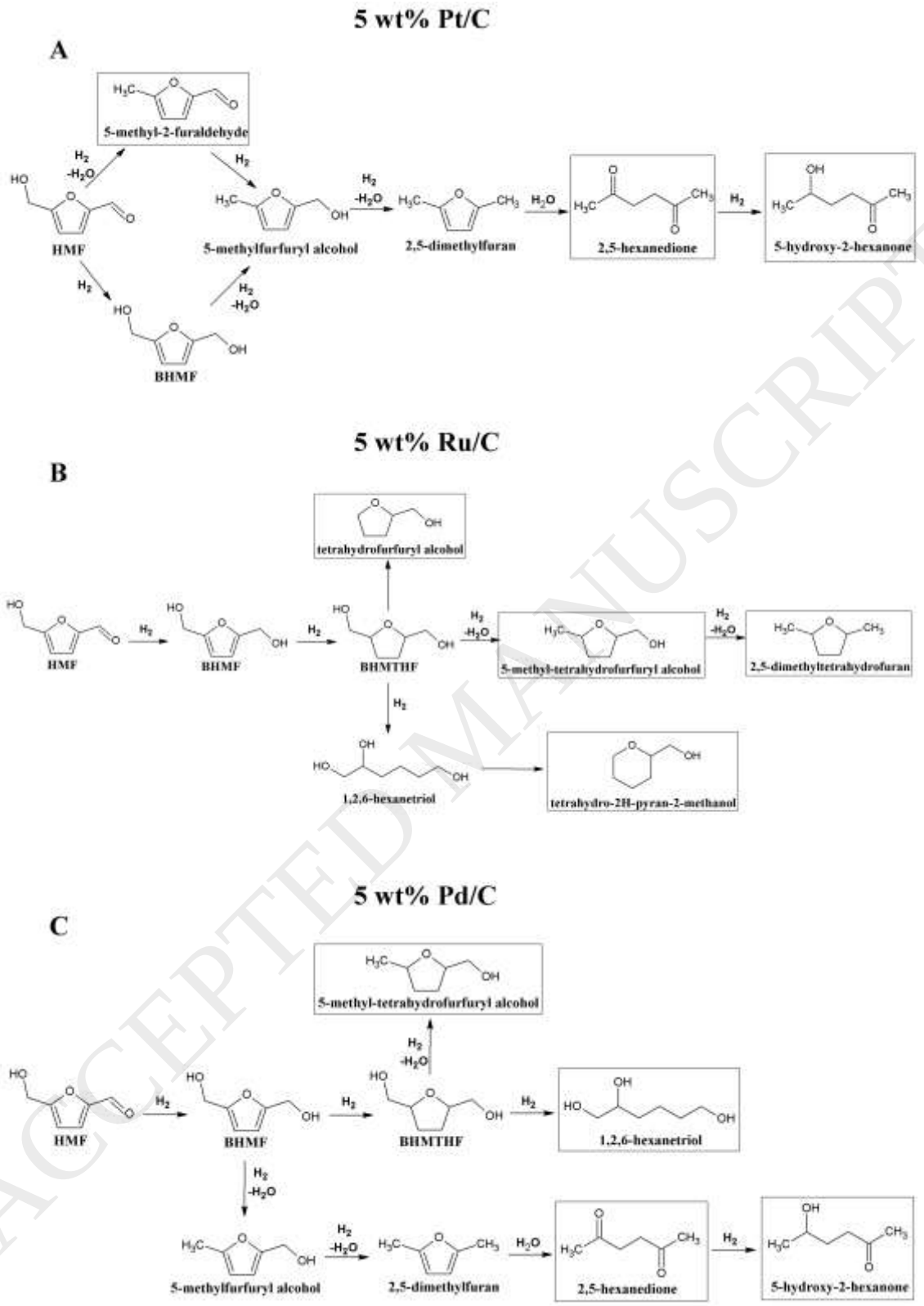

Scheme 2

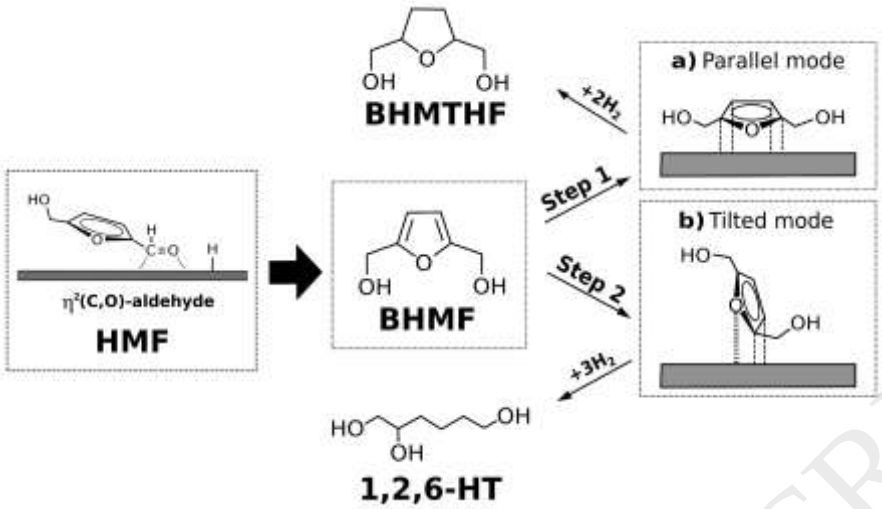

Figure 1

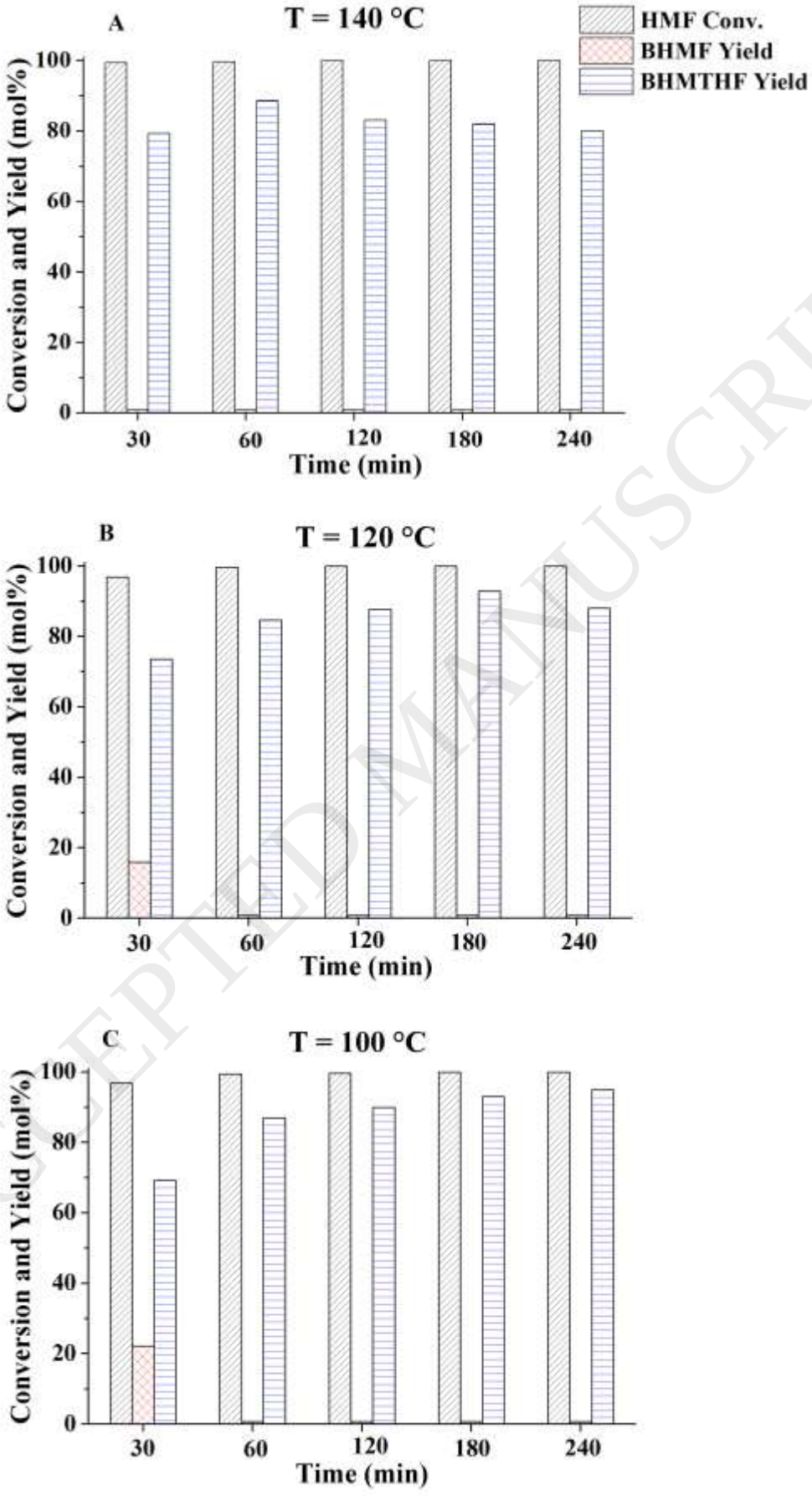

Figure 2

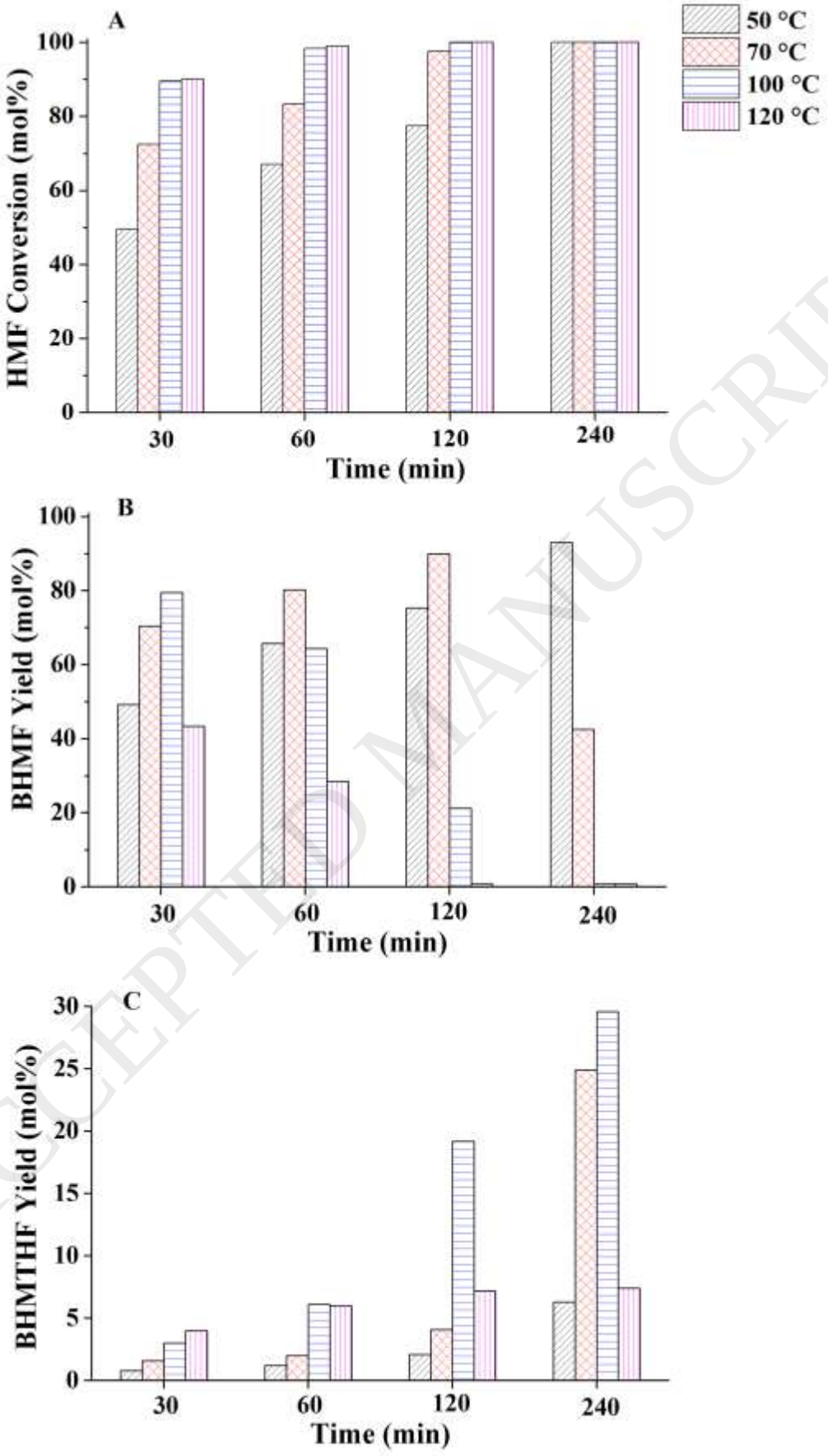

Figure 3

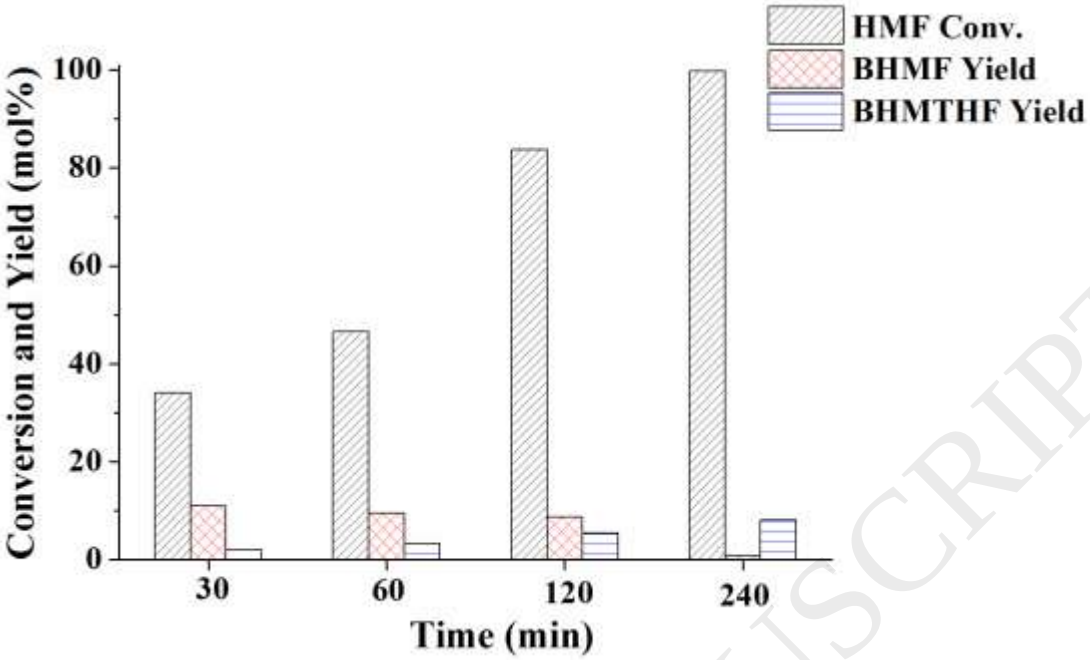

Figure 4

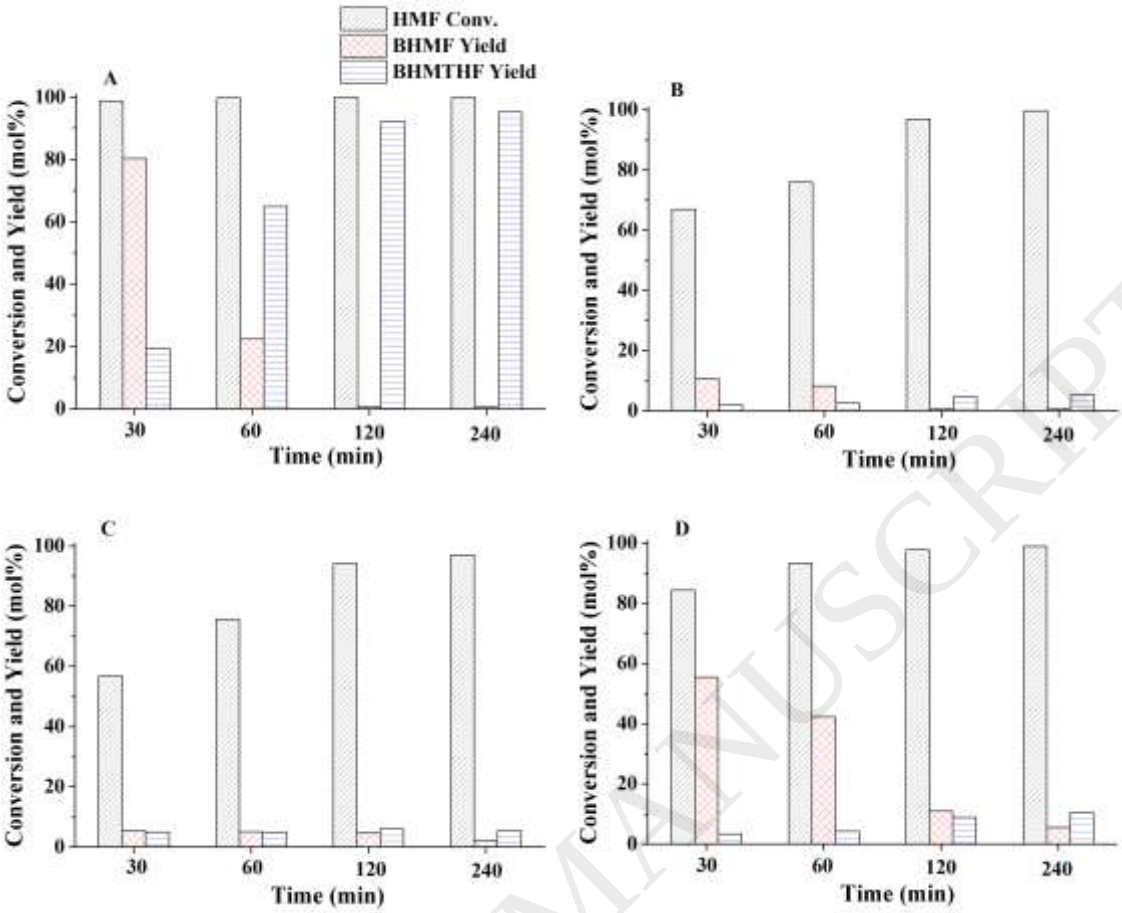

Figure 5

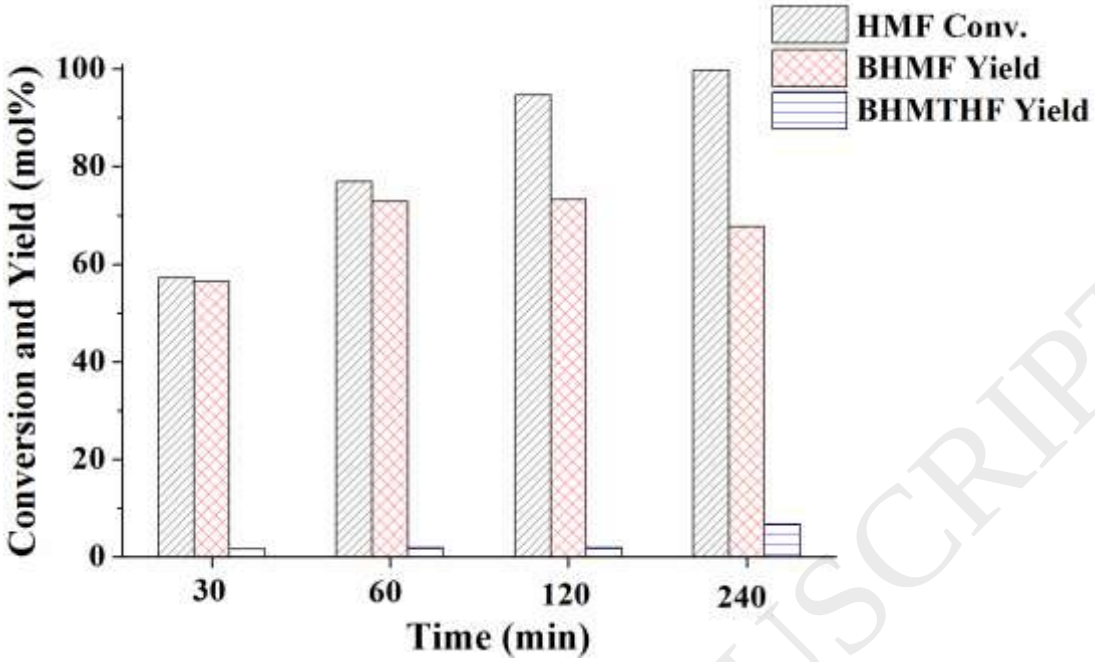

Figure 6

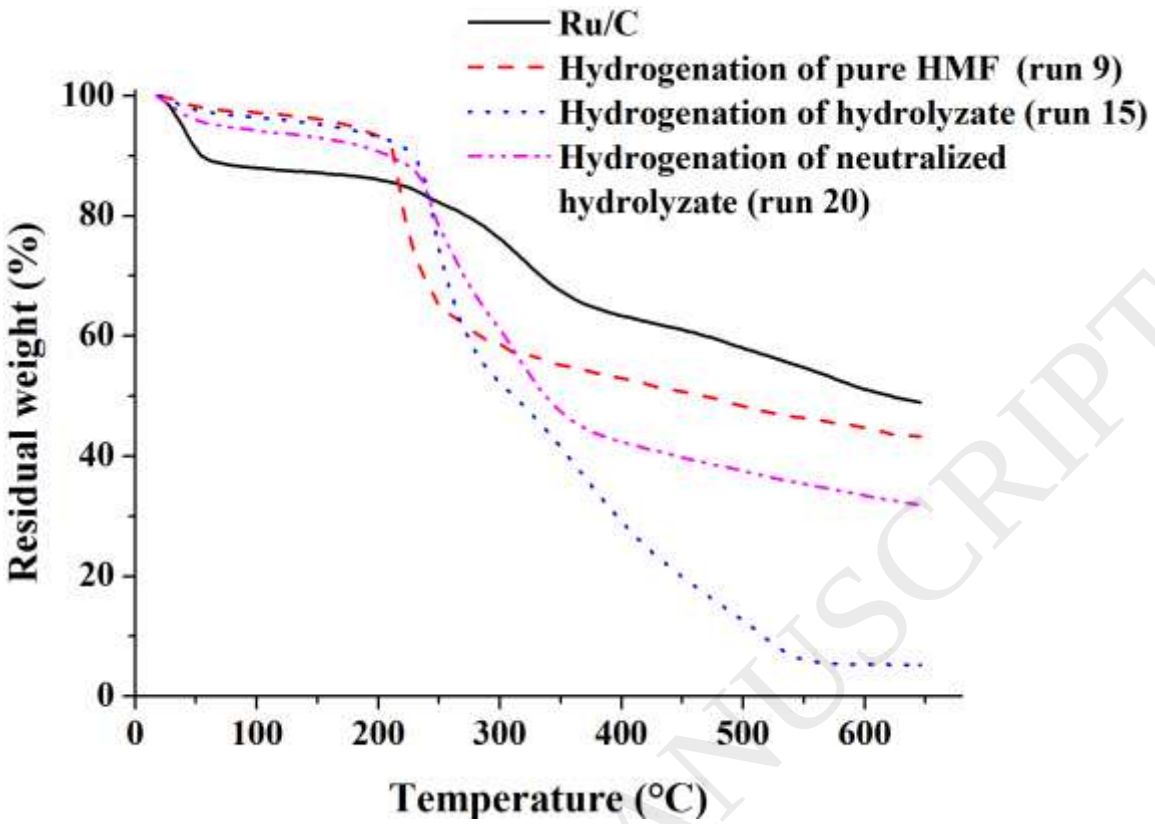

Figure 7

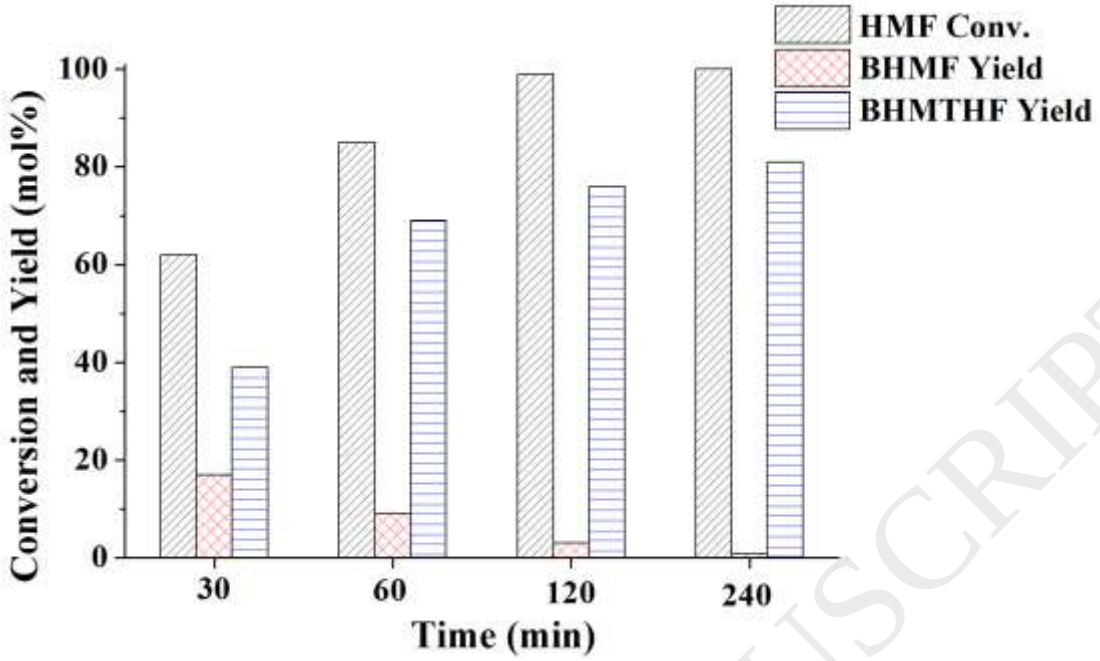

Figure 8

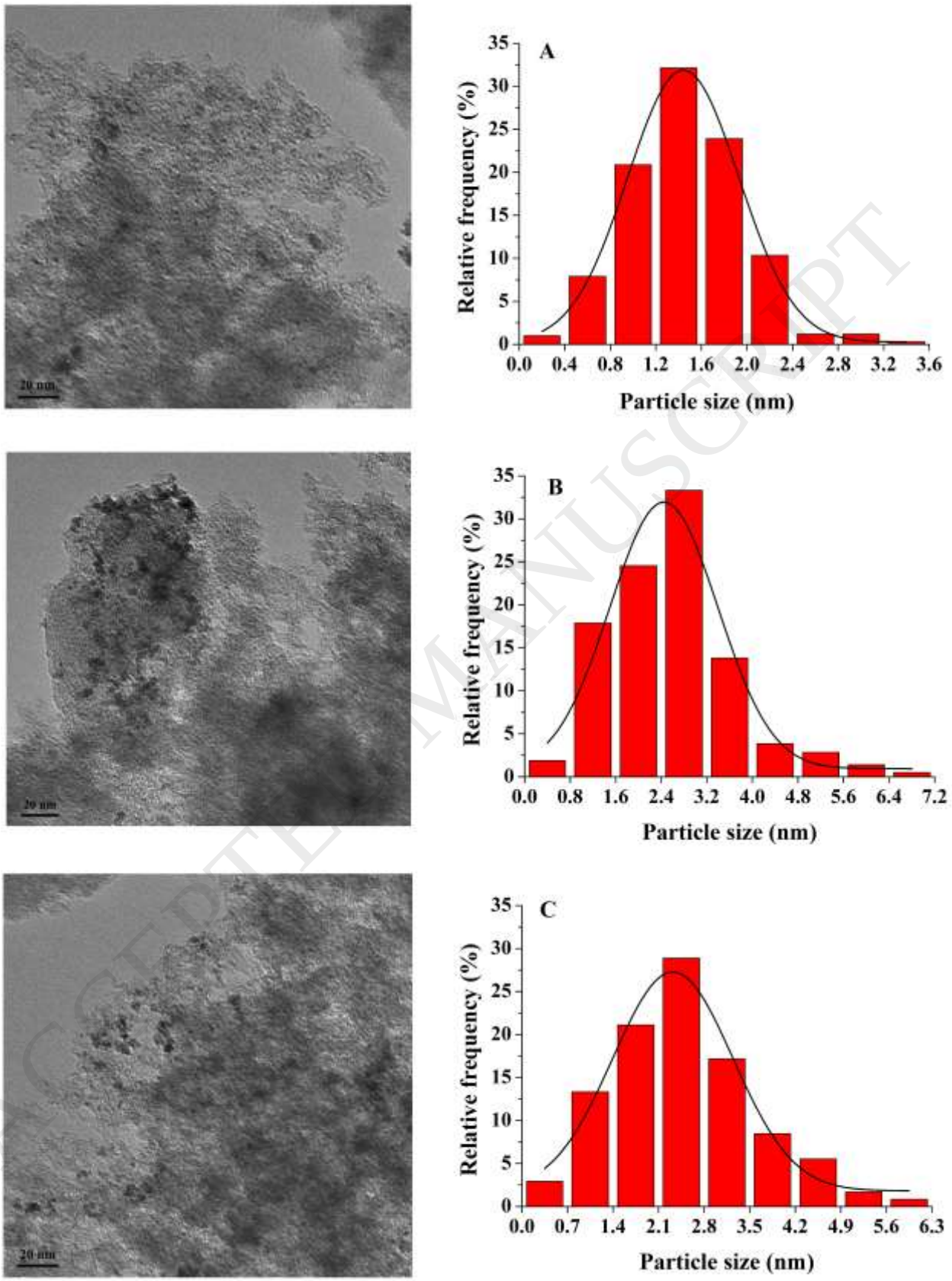

Figure 9